Mechanism of Aging of Mipafox−Inhibited Butyrylcholinesterase

ARTICLE *in* CHEMICAL RESEARCH IN TOXICOLOGY · APRIL 2007

Impact Factor: 3.53 · DOI: 10.1021/tx600310y · Source: PubMed

2 AUTHORS, INCLUDING:

Rudy J Richardson
University of Michigan
123 PUBLICATIONS **3,161** CITATIONS

SEE PROFILE

Mechanism of Aging of Mipafox-Inhibited Butyrylcholinesterase

Timothy J. Kropp[†] and Rudy J. Richardson*[,†,‡]

Toxicology Program, Department of Environmental Health Sciences, and Department of Neurology, The University of Michigan, Ann Arbor, Michigan 48109-2029

Received November 6, 2006

Elucidating mechanisms of aging of esterases inhibited by organophosphorus (OP) compounds is important for understanding toxicity and developing biomarkers of exposure to these agents. Aging has classically been thought to involve net loss of a single side group from the OP moiety of phosphylated esterases, rendering the enzyme refractory to reactivation. However, recent evidence has shown that acetylcholinesterase (AChE) and the catalytic domain of human neuropathy target esterase (NEST) undergo aging by alternative mechanisms following their inhibition with *N*,*N*′-diisopropylphosphorodiamidofluoridate (mipafox, MIP). This study was performed to determine whether MIP-inhibited butyrylcholinesterase (BChE) ages conventionally, by net loss of a single side group, or by an alternate route, e.g., reversible deprotonation or displacement of both isopropylamine groups, as recently observed for MIP-inhibited NEST and AChE, respectively. Diisopropylphosphorofluoridate (DFP), the phosphate analogue of the phosphoroamidate MIP, was used for comparison. Kinetic values for MIP against BChE were as follows: $k_i = (1.28 \pm 0.053) \times 10^6$ M^{-1} min^{-1}; $k_3 = 0.004\,15 \pm 0.000\,27$ min^{-1}; $k_4 = 0.008\,49 \pm 0.000\,99$ min^{-1}. Kinetic values for DFP against BChE were as follows: $k_i = (1.83 \pm 0.18) \times 10^6$ M^{-1} min^{-1}; $k_3 = 0.004\,88 \pm 0.000\,24$ min^{-1}; $k_4 = 0.0121 \pm 0.0028$ min^{-1}. Mass spectrometric studies revealed a mass shift of 123.4 ± 0.7 Da for the active-site peptide peak of aged DFP-inhibited BChE, corresponding to a monoisopropylphosphate adduct. Similarly, the analogous mass shift for aged MIP-inhibited BChE was 122.4 ± 0.7 Da, corresponding to a monoisopropylphosphoroamido adduct. Therefore, we conclude that the MIP−BChE conjugate ages by loss of a single isopropylamine group, in contrast to MIP-inhibited AChE or NEST.

Introduction

Some organophosphorus (OP)[1] compounds elicit cholinergic neurotoxicity by inhibiting synaptic acetylcholinesterase (AChE). In addition, inhibition and aging of neuropathy target esterase (NTE) by certain OP compounds leads to delayed neuropathy. Multiple other serine hydrolases are targets for OP compounds, but owing to a lack of understanding of their biological functions, the clinical significance of their inhibition or aging is incompletely understood. One such target protein is butyrylcholinesterase (BChE) (*1*, *2*).

As with other B-esterases, OP inhibition of BChE occurs by phosphylation of the active-site serine. The hydroxyl oxygen of the active-site serine attacks the phosphorus atom of the OP compound, displacing the primary leaving group and forming a covalent bond with the phosphyl moiety. Enzymatic activity can be restored only by nucleophilic displacement of the esterase from its phosphyl conjugate, which occurs slowly with water (spontaneous reactivation) and more rapidly with stronger nucleophiles, such as potassium fluoride (KF) or pyridine-2-aldoxime methiodide (2-PAM). However, the phosphylated enzyme may undergo aging, yielding a negatively charged adduct that is intractable to spontaneous, KF-, or 2-PAM-mediated reactivation (*3*).

Although phosphylation of BChE is not known to produce toxicity directly (*1*), this process is of considerable toxicological interest. For example, the resulting inhibition antagonizes the catalytic hydrolysis of natural and synthetic carboxylate esters as well as the stoichiometric inactivation of OP compounds that can be mediated by this enzyme (*4*). Moreover, owing to its presence in plasma, BChE phosphylation can serve as a convenient biomarker of OP compound exposure (*5*). By use of kinetic and mass spectrometric (MS) methods, it is possible to determine not only the degree of exposure but also the identity of the OP adduct on BChE or other target proteins (*6*−*8*). However, the extent of inhibition and chemical composition of the OP adduct can change over time, depending upon the rate of reactivation as well as the rate and nature of aging. Therefore, in order to make accurate predictions about the conjugates on BChE or other esterases resulting from OP compound exposures, it is important to elucidate the mechanisms of inhibitory and postinhibitory reactions (*9*−*11*).

One of the most extensively studied OP compounds is diisopropylphosphorofluoridate (DFP). The inhibition and aging reactions of several DFP-treated esterases have been thoroughly investigated. These studies have included AChE (*8*, *12*, *13*), BChE (*14*−*17*), NTE (*18*, *19*), and NTE catalytic domain (NEST) (*20*). Each of these DFP-inhibited esterases ages by net isopropyl loss, yielding an anionic monoisopropylphosphate moiety on the active-site serine. The aged DFP−esterase

* To whom correspondence should be addressed: Toxicology Program, Department of Environmental Health Sciences, The University of Michigan, 1420 Washington Heights, Ann Arbor, MI 48109-2029; tel 734-936-0769; fax 734-763-8095; e-mail rjrich@umich.edu.

† Toxicology Program, Department of Environmental Health Sciences.

‡ Department of Neurology.

[1] Abbreviations: AChE, acetylcholinesterase; BChE, butyrylcholinesterase; BTCh, butyrylthiocholine; DFP, diisopropylphosphorofluoridate; DTNB, 5,5′-dithiobis(2-nitrobenzoic acid); MIP, *N*,*N*′-diisopropylphosphorodiamidofluoridate (mipafox); MALDI, matrix-assisted laser desorption/ionization; MH^+, protonated molecule; NTE, neuropathy target esterase; NEST, human recombinant neuropathy target esterase (catalytic) domain; OP, organophosphorus; 2-PAM, pyridine-2-aldoxime methiodide; SELDI, surface-enhanced laser desorption/ionization; TOF, time-of-flight.

10.1021/tx600310y CCC: $37.00
Published on Web 02/27/2007

conjugates have been directly demonstrated by MS for AChE (*8*, *12*) and NEST (*20*), by X-ray crystallography for AChE (*13*) and BChE (*16*), and by NMR for BChE (*17*).

Less thoroughly studied than DFP is its phosphoroamidate analogue, *N*,*N*′-diisopropylphosphorodiamidofluoridate (mipafox, MIP). Given the structural similarities of DFP and MIP, and the fact that AChE inhibited by the phosphoroamidate, ethyl *N*,*N*-dimethylphosphoroamidocyanidate (tabun) ages by P−N bond scission (*11*), it would be reasonable to expect that MIP-inhibited serine esterases would age by displacement of an isopropylamine group. Nevertheless, from the studies that have been done, it is apparent that the aging of MIP-inhibited esterases is a less consistent process than that of DFP-inhibited esterases. For example, previous work yielded equivocal results, indicating that MIP-inhibited AChE and NTE might not undergo aging at all but instead form inherently nonreactivatable conjugates directly upon inhibition (*21*). However, recent kinetic and MS investigations have shown that whereas MIP-inhibited NEST does not age classically by side-group expulsion, it does age unconventionally by phosphoroamido deprotonation (*20*). Furthermore, consistent with ejection of dimethylamine in the aging of tabun-inhibited AChE (*11*), displacement of isopropylamine occurs during the aging of MIP-inhibited AChE (*12*). Remarkably, however, MIP-inhibited AChE loses both of its isopropylamine groups during aging to yield a simple phosphoserine adduct.

Thus, although the aging of MIP-inhibited BChE had not been investigated before the present study, based on the results from experiments on the aging of MIP-inhibited NEST and AChE, the reaction could be predicted to proceed either by deprotonation or by dual displacement of isopropylamine groups. However, given the similarities in AChE and BChE structure and catalytic mechanism (*4*) and their dissimilarities to NEST (*20*), it is more likely that the aging of MIP-inhibited BChE would proceed in a manner similar to that of MIP-inhibited AChE. Therefore, the present kinetic and MS investigation was carried out to test the hypothesis that MIP-inhibited BChE undergoes aging by the net loss of two isopropylamine groups, as previously reported for MIP-inhibited AChE (*12*). DFP-inhibited BChE was included for comparison and to confirm via kinetics and MS that its aging occurs by net loss of an isopropyl group, as predicted by molecular modeling (*14*) and shown by X-ray crystallography (*16*) and NMR (*17*). Equine (horse serum) BChE was used in this research because of its commercial availability, existing data for mechanisms of inhibition and aging with which to compare the results, and solubility without salts or detergents that interfere with MALDI/SELDI-TOF MS analysis (*6*, *7*). Moreover, in view of the high sequence identity of equine BChE with that of other species (e.g., 89% with human BChE) (*22*), it is expected that the results of the present study would have excellent predictive value for the mechanism of aging of MIP-inhibited BChE from other species.

Experimental Procedures

Chemicals and Enzymes. Equine (horse serum) BChE (stock C1057, lot 0112K70581), trypsin (stock T8658, lot 101K51042), and DFP (98% pure by gas chromatography, GC) were purchased from Sigma (St. Louis, MO). MIP was purchased from ChemSyn Laboratories (Lenexa, KS) (99% pure by HPLC). All other chemicals were the highest purity available and were obtained from commercial sources. **Caution:** *DFP and MIP are hazardous and should be handled carefully. These chemicals should be handled in a fume hood and weighed by difference in stoppered containers. Items contaminated with DFP or MIP should be soaked overnight in 1 M NaOH to inactivate the compounds before disposal.*

Kinetics. Residual activity of inhibited BChE was assayed in 0.10 M sodium phosphate buffer (pH 8.0 at 25 °C) by a modification of the method of Ellman et al. (*23*). Inhibitors were dissolved in acetone and diluted in phosphate buffer. Final acetone concentration was ≤1% (v/v), a solvent concentration shown in previous studies in our laboratory not to affect enzyme activity. Enzyme and inhibitor were preincubated for various measured times. At the end of each period, substrate solution containing butyrylthiocholine (BTCh) and 5,5′-dithiobis(2-nitrobenzoic acid) (DTNB) (final concentrations, BTCh 1.0 mM, DTNB 0.32 mM) was added. Activity was determined by measuring the change in absorbance at 412 nm over a 1−2 min period by use of a SPECTRAmax 340 microplate reader at 25 °C (Molecular Devices Corp., Sunnydale, CA). The apparent bimolecular rate constants of inhibition (k_i) for DFP and MIP against BChE were determined as previously described for other inhibitors (*6*).

Reactivation of inhibited BChE was carried out by incubating BChE with inhibitors at concentrations determined by kinetics to yield ∼90% inhibition in 10 min (MIP, 0.18 μM; DFP, 0.13 μM). Reactions were performed at 25 °C in pH 8.0 phosphate buffer. An aliquot of the enzyme solution was diluted 1:100 (v/v) in buffer alone or in buffer containing 200 mM KF or 200 μM 2-PAM, each at 25 °C. Aliquots were withdrawn at timed intervals from 0 to 18 h and assayed for activity as described above. The apparent first-order rate constants of reactivation (k_3) for spontaneous, KF-, or 2-PAM-mediated reactivation were determined according to methods described by Clothier et al. (*24*) and Jianmongkol et al. (*25*).

Aging was carried out similarly to reactivation by incubating enzymes with inhibitors at 25 °C for 10 min in pH 8.0 phosphate buffer to achieve ∼90% inhibition (MIP, 0.18 μM; DFP, 0.13 μM). Aliquots were then diluted 1:100 (v/v) with phosphate buffer effectively to stop the inhibition reaction. Both diluting buffers were without 2-PAM. The inhibited enzyme was then allowed to age for timed intervals from 0 to 18 h. At the end of each timed interval, an aliquot of inhibited enzyme solution was removed and incubated with 2-PAM (final concentration 100 μM) for 20 min at 25 °C before determination of residual enzyme activity. In parallel, the residual activity in the absence of 2-PAM was determined to serve as a control. Reactions were performed at 25 °C. Similar experiments performed in the presence of KF instead of 2-PAM showed no difference in the rate of aging (data not shown). The apparent first-order rate constants of aging (k_4) were determined as described by Clothier et al. (*24*) and Jianmongkol et al. (*25*).

Mass Spectrometry. Samples were prepared for MS studies in a manner similar to that described by Doorn et al. (*7*). BChE was incubated in 50 mM ammonium bicarbonate buffer (pH 8.0 at 25 °C) with concentrations of inhibitors (DFP or MIP) determined from kinetics studies to yield ∼90% inhibition in 10 min (MIP, 0.18 μM; DFP, 0.13 μM). Control samples of BChE were incubated with buffer only. One set of inhibited samples was subjected immediately after inhibition or control incubation to tryptic digestion (see below) in order to attempt detection of nonaged adducts. Another set of control or inhibited samples was allowed to incubate for 0.5, 1, 2, 4, 8, 24, and 168 h.

Control, inhibited, and aged samples were digested with trypsin as described by Doorn et al. (*7*). The sequence for equine (horse serum) BChE was obtained from the ESTHER database (http://bioweb.ensam.inra.fr/ESTHER/general?what=index) (*26*). The average masses of the tryptic digests of each sequence were predicted by use of the MS-Digest feature of ProteinProspector version 4.0.7 (http://prospector.ucsf.edu/) (*27*). By use of these tools, the tryptic digest peptide containing the active-site serine (shown in boldface type) and its associated *m*/*z* value (average mass) for the protonated molecule (MH^+) were predicted to be as follows: SVTLFGE**S**AGAASVSLHLLSPR (2200.52). Adduction of the active-site serine in this peptide with DFP, monoisopropyl DFP, MIP, monoisopropyl MIP, and phosphate would result in positive average *m*/*z* shifts of 164.15, 122.06, 162.17, 121.07, and 79.98, respectively. These *m*/*z* shifts account for the serine hydroxyl hydrogen that would be lost in the organophosphylation reaction.

Table 1. Kinetic Values for MIP- and DFP-Treated BChE Samples[a]

inhibitor	k_i (M^{-1} min^{-1})	k_3[b] (min^{-1})	k_4 (min^{-1})
MIP	$(1.28 \pm 0.05) \times 10^6$	$0.004\,15 \pm 0.000\,27$	$0.008\,49 \pm 0.000\,99$
DFP	$(1.83 \pm 0.18) \times 10^6$	$0.004\,88 \pm 0.000\,24$	0.0121 ± 0.0028

[a] Values are means ± SE ($n = 4$). [b] Values for spontaneous reactivation.

Surface-enhanced laser desorption/ionization time-of-flight MS (SELDI-TOF MS) is a modification of matrix-assisted laser desorption/ionization- (MALDI-) TOF MS. The SELDI or ProteinChip technique combines MALDI-TOF MS with retentive chromatographic separation on the MALDI plate (*28*). Aliquots (1−3 μL) of nondiluted and 1:10 and 1:100 (v/v) diluted peptide mixture in 50 mM ammonium bicarbonate (pH 8.0 at 25 °C) were deposited on gold, H4 (hydrophobic), and NP1 (hydrophilic) ProteinChip plates (Ciphergen Biosystems, Inc., Fremont, CA) for chromatographic treatment or no treatment. No treatments of the gold plate were made. Samples for treatment that were deposited on H4 plates were prewashed with acetonitrile and incubated in a humidity chamber at room temperature for 20 min. The samples were then washed 3 times with 5 μL of 20% (v/v) acetonitrile. Samples for treatment that were deposited on NP1 plates were incubated for 30 min at room temperature in a humidity chamber. The samples were then washed three times with 2 μL of water. All samples were dried at 50 °C, and 1 μL of a 50% (v/v) acetonitrile/50% (v/v) 1% trifluoroacetic acid (w/v) solution saturated with the matrix, α-cyano-4-hydroxycinnamic acid, was deposited on top of the samples, which were then dried at 50 °C.

A PBS-II SELDI-TOF MS instrument (Ciphergen Biosystems, Inc., Fremont, CA) equipped with a nitrogen laser (337 nm, 4 ns pulse width) was used to acquire mass spectra. Laser intensities used for each experiment were within 20% of the average, but laser intensities for a given experiment were adjusted as required to detect potential adducted peaks. Analysis was carried out with an acceleration voltage of 20 kV, and 100−200 laser shots were averaged for each spectrum. The instrument was externally calibrated before each experiment in the following manner. A solution of 1 mg/mL equine BChE was digested with trypsin and the predicted peptide map was obtained as described above. Aliquots (1 μL) of BChE peptide digest were plated as described as above. After drying, the sample spot was spiked with 1 μL of a solution containing 1 mg/mL dynorphin A and 1 mg/mL human angiotensin-I (Ciphergen Biosystems, Inc., Fremont, CA) in 50 mM ammonium bicarbonate solution (pH 8.0 at 25 °C) and analyzed as described above. The predicted tryptic digest peaks, along with peaks corresponding to dynorphin A and human angiotensin-I, were used to obtain the most accurate calibration for the BChE experimental samples. Subsequently, internal calibration was performed by use of predicted peaks from tryptic digests of trypsin and BChE other than the BChE active-site peptide or its predicted adducts. Peptide map coverage of 49% was obtained for digested BChE (data not shown). Representative spectra from different experiments displayed in Figure 1 are from unfractionated samples deposited on H4 chips with no chromatographic treatments.

Statistical Analysis. Significance of differences between observed and theoretical *m*/*z* values was assessed by independent two-tailed *t*-tests with $p < 0.05$ being regarded as significant. All plots, regressions, and *t*-tests were carried out with GraphPad versions 3.02 and 4.02 for Windows, GraphPad Software, Inc. (San Diego, CA).

Results

The results of the inhibitory and postinhibitory kinetics determinations are displayed in Table 1. From the k_i values, it can be seen that MIP was found to be approximately 1.4 times less potent than DFP as an inhibitor of BChE. Results of investigation of the spontaneous reactivation rate constants (k_3) are also shown in Table 1. In addition, it was found that MIP-inhibited BChE was reactivated in the presence of 2-PAM with a k_3 of 0.0293 ± 0.0118 min^{-1} and in the presence of KF with a k_3 of 0.0221 ± 0.0074 min^{-1}. DFP-inhibited BChE was reactivated in the presence of 2-PAM with a k_3 of 0.0521 ± 0.0129 min^{-1} and in the presence of KF with a k_3 of 0.0456 ± 0.0162 min^{-1}. It can be seen from Table 1 that the rate constants of aging (k_4) were about 2- and 2.5-fold higher than the spontaneous k_3 for MIP- and DFP-inhibited BChE, respectively.

Table 2. Differences in Average Mass of MH^+ Ions of Active-Site Peptides from Nonaged or Aged Adducts of BChE with DFP or MIP[a]

data type	Δ*m* DFP nonaged	Δ*m* DFP aged	Δ*m* MIP nonaged	Δ*m* MIP aged
observed	165.0 ± 0.5	123.4 ± 0.7	162.9 ± 0.4	122.4 ± 0.7
theoretical	164.2	122.1	162.2	121.1

[a] Values are means ± SE ($n \geq 10$). The *m*/*z* values (average mass) for the MH^+ ion of the unreacted tryptic digest peptide containing the active-site Ser are 2200.5 ± 0.1 (observed) and 2200.5 (theoretical). Theoretical values of Δ*m* (*m*/*z*) take into account the average mass of the Ser hydroxyl proton that is lost in the organophosphylation reaction. Observed *m*/*z* values were not different from corresponding theoretical values ($p > 0.1$).

The results for the SELDI-TOF MS experiments are contained in Table 2 and representative spectra are displayed in Figure 1. All OP treatment-dependent mass shifts were accounted for in the MIP- and DFP-treated samples.

MS studies of MIP-inhibited BChE showed two time-dependent shifts in the peak corresponding to the control BChE active-site peptide (2200.5 ± 0.1 *m*/*z*; labeled 2200.5 *m*/*z* in the representative spectrum reproduced in Figure 1A,D). The first new peak (2363.4 ± 0.4 *m*/*z*; labeled 2363.7 *m*/*z* in the representative spectrum shown in Figure 1B) was seen at 0, 0.5, 1, and 2 h time points and corresponds to the active-site peptide adducted by the intact MIP inhibition product, an *N*,*N*′-diisopropylphosphorodiamido adduct. The second new peak (2322.9 ± 0.7 *m*/*z*; labeled 2322.9 *m*/*z* in the representative spectrum shown in Figure 1C) appeared at time points from 1 to 168 h. This second peak corresponds to an aged MIP-inhibited BChE active-site peptide, in this case, a monoisopropylphosphoroamido adduct. No peaks corresponding to a phosphate-adducted BChE active-site peptide were detected at any time point.

MS studies of DFP-inhibited BChE showed two time-dependent shifts in the peak corresponding to the control BChE active-site peptide (2200.5 ± 0.1 *m*/*z*; labeled 2200.5 *m*/*z* in the representative spectrum reproduced in Figure 1A,D). The first new peak (2365.5 ± 0.5 *m*/*z*; labeled 2365.7 *m*/*z* in the representative spectrum in Figure 1E) was seen at 0, 0.5, and 1 h time points and corresponds to the active-site peptide adducted by the intact DFP inhibition product, a diisopropylphosphoryl adduct. The second peak (2324.9 ± 0.7 *m*/*z*; labeled 2323.7 *m*/*z* in the representative spectrum in Figure 1F) appeared at time points from 0.5 to 18 h. This second peak corresponds to an aged DFP-inhibited BChE active-site peptide, in this case, a monoisopropylphosphoryl-adducted active site.

Different peak coverage was found for different retentive chromatographic treatments of SELDI chips; cumulative peptide map coverage for all treatments for BChE was 49%. As noted in Figure 1, all spectra contained some prominent peaks that did not correspond to those predicted for BChE, trypsin autolysis, or keratin contamination. Because equine serum BChE is known to be highly glycosylated (up to 24% of its mass) (*22*, *29*), it is possible that these uncharacterized peaks represent glycosylated peptides. However, given that assignments of these peaks were not needed for analysis of changes in the peaks corresponding to the BChE active-site peptide and its OP adducts, this possibility was not investigated further. Sodium

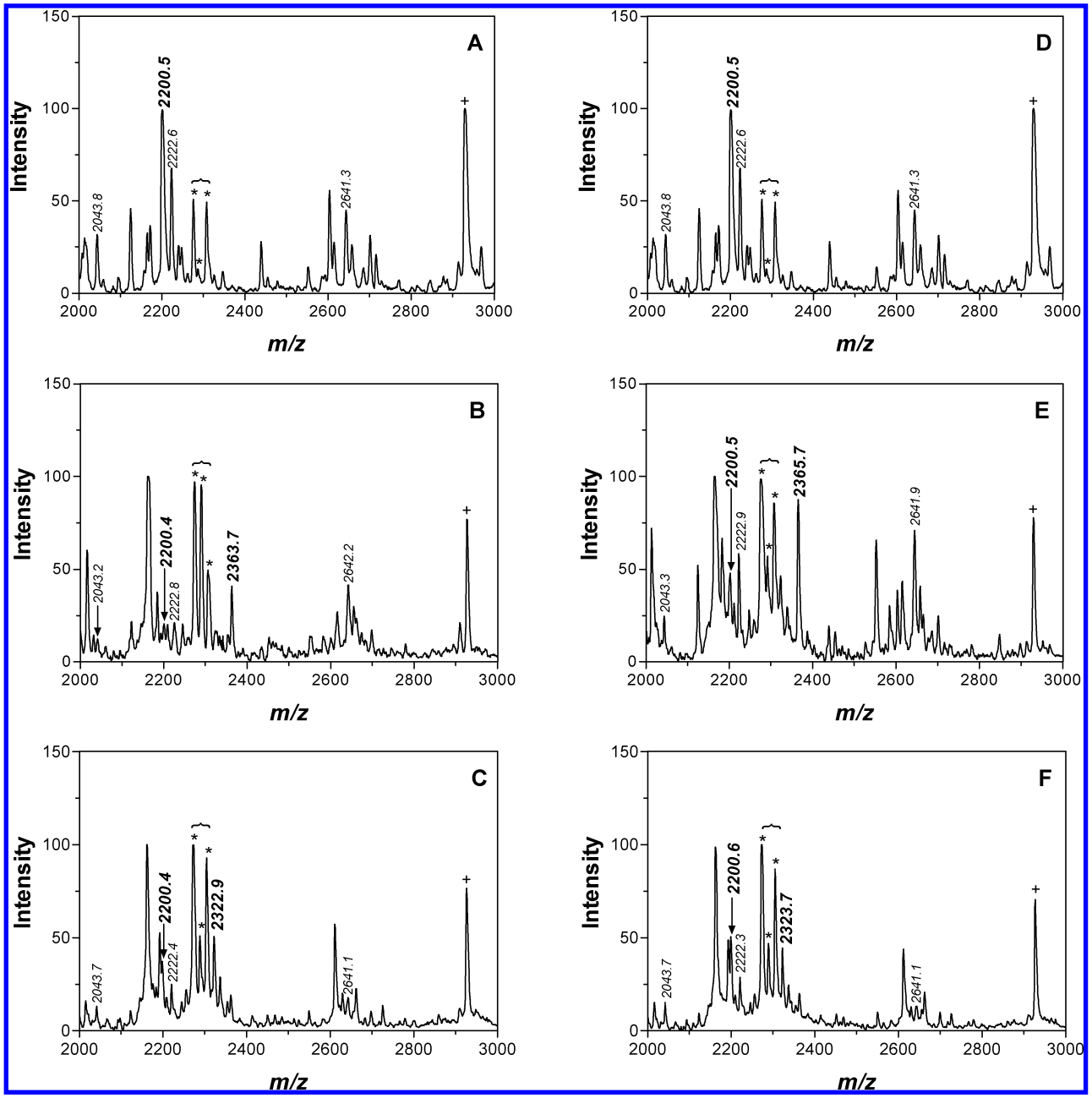

Figure 1. Representative SELDI-TOF MS spectra of unfractionated tryptic digests of BChE samples from each experiment. (A) Control BChE. Peak with *m*/*z* of 2200.5 represents the unmodified active-site peptide containing the catalytic Ser. (B) BChE-MIP. Peak with *m*/*z* of 2363.7 represents the active-site peptide with an *N*,*N*′-diisopropylphosphorodiamido adduct. (C) Aged BChE-MIP. Peak with *m*/*z* of 2322.9 represents the active-site peptide with an *N*-isopropylphosphoroamido group adduct. (D) Control BChE (duplicate of panel A for ease of comparison). Peak with *m*/*z* of 2200.5 represents the unmodified active-site peptide containing the catalytic Ser. (E) BChE-DFP. Peak with *m*/*z* of 2365.7 represents the active-site peptide with a diisopropylphosphate adduct. (F) Aged BChE-DFP. Peak with *m*/*z* of 2323.7 represents the active-site peptide with a monoisopropylphosphate adduct. Note: Laser intensities were varied for each spectrum to ensure detection of peaks arising from OP treatment. Numbers in lightface type indicate observed *m*/*z* values corresponding to predicted BChE peaks other than the active-site peak or its OP adducts. Numbers in boldface type indicate observed *m*/*z* values corresponding to predicted BChE active-site peaks or OP adducts. Bracketed peaks labeled with asterisks (*m*/*z* 2274.0, 2289.2, and 2306.2) and the peak labeled + (*m*/*z* 2928.0) were not predicted BChE, trypsin autolysis, or keratin contamination peaks but were consistently found in all spectra.

adducts of predicted peptides were identified in some spectra and were found to be independent of OP incubation. No OP treatment-dependent mass shifts were found other than those described above.

Discussion

The k_i values for MIP and DFP show relatively similar inhibitory potencies of MIP and DFP against equine BChE. Moreover, the 30-min pI_{50} values of 7.74 and 7.90 derived from the k_i values for MIP and DFP, respectively, compare favorably with the 30-min pI_{50} values of 7.42 and 8.18 for MIP and DFP, respectively, reported by Aldridge and Reiner (*3*).

This investigation is the first to report aging and reactivation rate constants for MIP- and DFP-inhibited equine BChE. The MIP- and DFP-inhibited BChE rate constants of spontaneous reactivation were similar, with $t_{1/2}$ values of 167 ± 11 and 142 ± 7.0 min, respectively ($t_{1/2} = 0.693/k_3$). The rates of aging for MIP- and DFP-inhibited BChE were over 2-fold faster than the associated rates of spontaneous reactivation, with aging $t_{1/2}$ values of 81.6 ± 9.5 and 57.2 ± 12.2 min, respectively. It is

Scheme 1. Pathways of Inhibition and Aging of MIP for Three Serine Hydrolases: (A) NEST, (B) AChE, and (C) BChE[a]

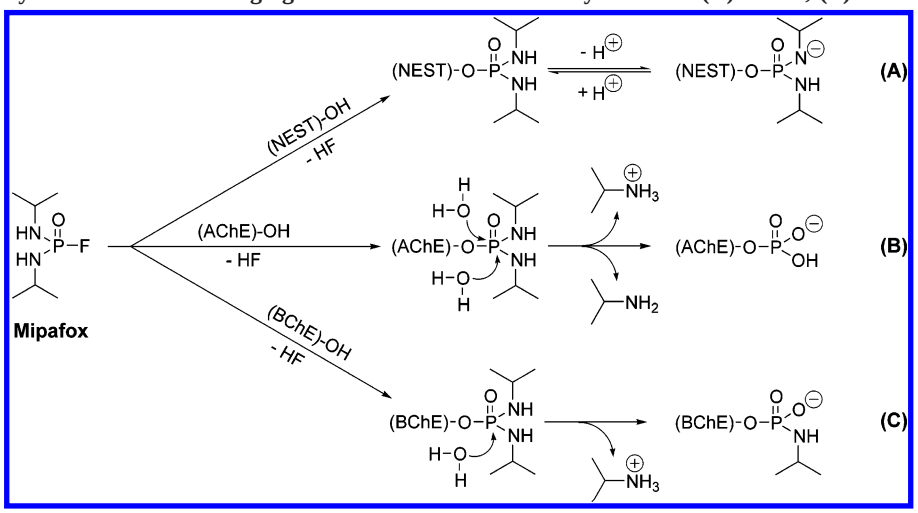

[a] References: (A) NEST (*20*); (B) AChE (*12*); (C) BChE (present work). Inhibition of each serine hydrolase occurs by nucleophilic attack of the Ser hydroxyl on the phosphorus, displacing the primary leaving group, fluoride, and yielding an *N*,*N*′-diisopropylphosphorodiamido adduct, which then undergoes aging by a different mechanism for each enzyme. Although the exact mechanisms (S_N1 or S_N2) of aging for MIP-inhibited AChE and BChE require definitive elucidation, results to date are consistent with S_N2 dual (AChE) or single (BChE) displacement of isopropylamine by water as shown here. The charge of each aged moiety is shown as expected for pH 8.0.

noteworthy that the $t_{1/2}$ value derived from the k_4 value reported here for DFP-inhibited equine BChE is in excellent agreement with the previously reported $t_{1/2}$ value of ~60 min for DFP-inhibited human BChE (*14*, *15*).

MS results confirm that DFP-inhibited BChE ages in a time-dependent manner, yielding a monoisopropylphosphoryl adduct on the active-site peptide, as previously predicted by kinetics, site-directed mutagenesis, and molecular modeling (*14*, *15*) and shown by X-ray crystallography (*16*) and NMR (*17*).

For MIP-inhibited BChE, the MS results show that aging yields neither an intact *N*,*N*′-diisopropylphosphoroamido adduct, as for MIP-inhibited NEST (*20*), nor a simple phosphate adduct, as in MIP-inhibited AChE (*12*). Instead, MIP-inhibited BChE ages similarly to DFP-inhibited BChE, by net loss of a single side group, yielding an *N*-monoisopropylphosphoroamido adduct as shown for BChE in Scheme 1. Thus, the working hypothesis for the present work was refuted. Accordingly, despite the similarities between AChE and BChE in structure and catalytic machinery (*4*), the differences that have also been noted between the active sites of these two enzymes are evidently sufficient to result in different mechanisms of aging when inhibited by MIP.

The presence of the *N*-monoisopropylphosphoroamido conjugate after aging of MIP-inhibited BChE indicates that aging occurs by scission of a P−N bond, as found previously for AChE inhibited by tabun (*11*) or MIP (*12*). The P−N bond scission likely occurs by acid-catalyzed hydrolysis, which could proceed in one of two ways (*30*). The first is a direct S_N2 substitution of the isopropylamine group by water. The second is a two-step S_N1 addition−elimination reaction with a proton addition to the nitrogen and subsequent attack on the phosphorus by water, which leads to the elimination of the isopropylamine group. In both cases, the isopropylamine group is ultimately replaced by water and the methods employed here could not distinguish between the two mechanisms.

It is remarkable that the aging of MIP-inhibited AChE, BChE, and NEST proceeds in three distinct ways as shown in Scheme 1. This finding is even more surprising, given that aging is different between the highly homologous and structurally similar enzymes AChE and BChE (*4*). The relative identities and/or positions of residues that stabilize the aged and nonaged OP−esterase adduct, as well as those that facilitate the aging process, may differ among these esterases. Indeed, human BChE is known to age faster than *Torpedo californica* AChE (TcAChE) for diethyl and diisopropyl phosphoryl adducts (*16*), possibly due to His438 in human BChE creating a more favorable environment for aging than that of His440 in TcAChE (*13*). Once aging occurs by single side-group loss, the aged AChE contains two short strong hydrogen bonds from His440, whereas aged BChE contains only one bond from His438 (*31*, *32*). It is possible that this slight conformational difference in the catalytic His confers sufficient extra stability on the *N*-monoisopropylphosphoroamido of AChE compared to that of BChE to enable loss of the second side group. In any event, the present study underscores the need to investigate further the molecular mechanisms of inhibition and aging of different OP compounds against their various esterase targets. For example, more needs to be known about the distinctive molecular topologies of the active sites of AChE, BChE, and NEST that give rise to different mechanisms of aging when these esterases are inhibited by MIP.

Moreover, the diversity of phosphoroamidate-inhibited esterase aging mechanisms relative to those of homologous phosphate analogues presents an opportunity to employ comparisons between these two and other classes of inhibitors in future studies of aging mechanisms.

It is interesting to note that while the aged adducts of MIP-inhibited AChE, BChE, and NEST are distinct from each other, the aged conjugates of DFP-inhibited AChE, BChE, and NEST are the same. Apart from its mechanistic interest, this systematic difference is of great practical importance in determining appropriate biomarkers of OP compound exposure. To date, relatively few esterase adducts of OP compounds have been directly analyzed by MS. Further study will not only augment the database of confirmed OP adducts but also enhance the prediction of adducts through a better understanding of structure−activity relationships. While additional investigation using multiple approaches is needed to guide the analysis of OP conjugates with target proteins, MS has proved to be an effective technique for identifying and quantifying adducts. Some of the challenges ahead include the development of strategies for identifying protein adducts from one or more compounds in complex samples such as human plasma or whole blood.

However, such work has begun and includes methods for liberating the adduct from proteins to detect small molecules (*33*−*37*), direct identification of protein conjugates (*5*, *38*, *39*), or conversion of variously phosphylated BChE active-site peptides to a common tagged peptide (*40*)

In summary, the kinetic and MS data presented here show that aging of MIP-inhibited BChE occurs by net loss of a single isopropylamine group, in contrast to the aging by net loss of both isopropylamine groups from MIP-inhibited AChE (*12*) or deprotonation of a phosphoroamido nitrogen from MIP-inhibited NEST (*20*).

Acknowledgment. We thank Dr. Robert Christner for technical assistance and helpful discussions. This material is based upon work supported in part by the U.S. Army Research Laboratory and the U.S. Army Research Office under Grant DAAD19-02-1-0388.

References

(1) Thompson, C. M., and Richardson, R. J. (2004) Anticholinesterase insecticides. In *Pesticide Toxicology and International Regulation* (Marrs, T. C., and Ballantyne, B., Eds.) pp 89−127, John Wiley and Sons, Ltd., Chichester, U.K.

(2) Casida, J. E., and Quistad, G. B. (2005) Serine hydrolase targets of organophosphorus toxicants. *Chem.-Biol. Interact. 157*−*158*, 277−283.

(3) Aldridge, W. N., and Reiner, R. E. (1972) *Enzyme Inhibitors as Substrates: Interactions of Esterases with Esters of Organophosphorus and Carbamic Acids*. North-Holland Publishing Company, Amsterdam.

(4) Nicolet, Y., Lockridge, O., Masson, P., Fontecilla-Camps, J. C., and Nachon, F. (2003) Crystal structure of human butyrylcholinesterase and of its complexes with substrate and products. *J. Biol. Chem. 278*, 41141−41147.

(5) Fidder, A., Hulst, A. G., Noort, D., de Ruiter, R., van der Schans, M. J., Benschop, H. P., and Langenberg, J. P. (2002) Retrospective detection of exposure to organophosphorus anti-cholinesterases: mass spectrometric analysis of phosphylated human butyrylcholinesterase. *Chem. Res. Toxicol. 15*, 582−590.

(6) Doorn, J. A., Talley, T. T., Thompson, C. M., and Richardson, R. J. (2001) Probing the active sites of butyrylcholinesterase and cholesterol esterase with isomalathion: conserved stereoselective inactivation of serine hydrolases structurally related to acetylcholinesterase. *Chem. Res. Toxicol. 14*, 807−813.

(7) Doorn, J. A., Schall, M., Gage, D. A., Talley, T. T., Thompson, C. M., and Richardson, R. J. (2001) Identification of butyrylcholinesterase adducts after inhibition with isomalathion using mass spectrometry: difference in mechanism between (1*R*)- and (1*S*)-stereoisomers. *Toxicol. Appl. Pharmacol. 176*, 73−80.

(8) Jennings, L. L., Malecki, M., Komives, E. A., and Taylor, P. (2003) Direct analysis of the kinetic profiles of organophosphate−acetylcholinesterase adducts by MALDI-TOF mass spectrometry. *Biochemistry 42*, 11083−11091.

(9) Doorn, J. A., Gage, D. A., Schall, M., Talley, T. T., Thompson, C. M., and Richardson, R. J. (2000) Inhibition of acetylcholinesterase by (1*S*,3*S*)-isomalathion proceeds with loss of thiomethyl: kinetic and mass spectral evidence for an unexpected primary leaving group. *Chem. Res. Toxicol. 13*, 1313−1320.

(10) Doorn, J. A., Thompson, C. M., Christner, R. B., and Richardson, R. J. (2003) Stereoselective inactivation of Torpedo californica acetylcholinesterase by isomalathion: inhibitory reactions with (1*R*)- and (1*S*)-isomers proceed by different mechanisms. *Chem. Res. Toxicol. 16*, 958−965.

(11) Elhanany, E., Ordentlich, A., Dgany, O., Kaplan, D., Segall, Y., Barak, R., Velan, B., and Shafferman, A. (2001) Resolving pathways of interaction of covalent inhibitors with the active site of acetylcholinesterases: MALDI-TOF/MS analysis of various nerve agent phosphyl adducts. *Chem. Res. Toxicol. 14*, 912−918.

(12) Kropp, T. J., and Richardson, R. J. (2006) Aging of mipafox-inhibited human acetylcholinesterase proceeds by displacement of both isopropylamine groups to yield a phosphate adduct. *Chem. Res. Toxicol. 19*, 334−339.

(13) Millard, C. B., Kryger, G., Ordentlich, A., Greenblatt, H. M., Harel, M., Raves, M. L., Segall, Y., Barak, D., Shafferman, A., Silman, I., and Sussman, J. L. (1999) Crystal structures of aged phosphonylated acetylcholinesterase: nerve agent reaction products at the atomic level. *Biochemistry 38*, 7032−7039.

(14) Masson, P., Fortier, P. L., Albaret, C., Froment, M. T., Bartels, C. F., and Lockridge, O. (1997) Aging of di-isopropyl-phosphorylated human butyrylcholinesterase. *Biochem. J. 327*, 601−607.

(15) Masson, P., Froment, M. T., Bartels, C. F., and Lockridge, O. (1997) Importance of aspartate-70 in organophosphate inhibition, oxime reactivation and aging of human butyrylcholinesterase. *Biochem. J. 325*, 53−61.

(16) Nachon, F., Asojo, O. A., Borgstahl, G. E. O., Masson, P., and Lockridge, O. (2005) Role of water in aging of human butyrylcholinesterase inhibited by echothiophate: The crystal structure suggests two alternative mechanisms of aging. *Biochemistry 42*, 1154−1162.

(17) Segall, Y., Waysbort, D., Barak, D., Ariel, N., Doctor, B. P., Grunwald, J., and Ashani, Y. (1993) Direct observation and elucidation of the structures of aged and nonaged phosphorylated cholinesterase by ^{31}P NMR spectroscopy. *Biochemistry 32*, 13441−13450.

(18) Williams, D. G. (1983) Intramolecular group transfer is a characteristic of neurotoxic esterase and is independent of the tissue source of the enzyme. A comparison of the aging behaviour of di-isopropyl phosphorofluoridate-labeled proteins in brain, spinal cord, liver, kidney and spleen from hen and in human placenta. *Biochem. J. 209*, 817−829.

(19) Williams, D. G., and Johnson, M. K. (1981) Gel-electrophoretic identification of hen brain neurotoxic esterase, labeled with tritiated di-isopropyl phosphorofluoridate. *Biochem. J. 199*, 323−333.

(20) Kropp, T. J., Glynn, P., and Richardson, R. J. (2004) The mipafox-inhibited catalytic domain of human neuropathy target esterase ages by reversible proton loss. *Biochemistry 43*, 3716−3722.

(21) Milatovic, D., and Johnson, M. K. (1993) Reactivation of phosphoramidated acetylcholinesterase and neuropathy target esterase by treatment of inhibited enzyme with potassium fluoride. *Chem.-Biol. Interact. 87*, 425−430.

(22) Wierdl, M., Morton, C. L., Danks, M. K., and Potter, P. M. (2000) Isolation and characterization of a cDNA encoding a horse liver butyrylcholinesterase. Evidence for CPT-11 drug activation. *Biochem. Pharmacol. 59*, 773−781.

(23) Ellman, G., Courtney, K. D., Andres, V., Jr., and Featherstone, R. M. (1961) A new and rapid colorimetric determination of acetylcholinesterase activity. *Biochem. Pharmacol. 7*, 88−95.

(24) Clothier, B., Johnson, M. K., and Reiner, E. (1981) Interaction of some trialkyl phosphorothiolates with acetylcholinesterase: characterization of inhibition, aging and reactivation. *Biochim. Biophys. Acta 660*, 306−316.

(25) Jianmongkol, S., Marable, B. R., Berkman, C. W., Tally, T. T., Thompson, C. M., and Richardson, R. J. (1999) Kinetic evidence for different mechanisms of acetylcholinesterase inhibition by (1*R*)- and (1*S*)-stereoisomers of isomalathion. *Toxicol. Appl. Pharmacol. 155*, 43−53.

(26) Cousin, X., Hotellier, T., Giles, K., Toutant, J. P., and Chatonnet, A. (1998) aCHEdb: the database system for ESTHER, the α/β fold family of proteins and the cholinesterase gene server. *Nucleic Acids Res. 26*, 226−228.

(27) Clauser, K. R., Baker, P. R., and Burlingame, A. L. (1999) Role of accurate mass measurement (±10 ppm) in protein identification strategies employing MS or MS/MS and database searching. *Anal. Chem. 71*, 2871.

(28) Issaq, H. J., Veenstra, T. D., Conrads, T. P., and Felshow, D. (2002) The SELDI-TOF MS approach to proteomics: protein profiling and biomarker identification. *Biochem. Biophys. Res. Commun. 292*, 587−592.

(29) Saxena, A., Raveh, L., Ashani, Y., and Doctor, B. P. (1997) Structure of glycan moieties responsible for the extended circulatory life time of fetal bovine serum acetylcholinesterase and equine serum butyrylcholinesterase. *Biochemistry 36*, 7481−7489.

(30) Eto, M. (1979) *Organophosphorus Pesticides: Organic and Biological Chemistry*. CRC Press, Boca Raton, FL.

(31) Viragh, C., Harris, T. K., Reddy, P. M., Massiah, M. A., Mildvan, A. S., and Kovach, I. M. (2000) NMR evidence for a short, strong hydrogen bond at the active site of a cholinesterase. *Biochemistry 39*, 16200−16205.

(32) Massiah, M. A., Viragh, C., Reddy, P. M., Kovach, I. M., Johnson, J., Rosenberry, T. L., and Mildvan, A. S. (2001) Short, strong hydrogen bonds at the active site of human acetylcholinesterase: proton NMR studies. *Biochemistry 40*, 5682−5690.

(33) Jakubowski, E. M., Heycamp, L. S., Durst, H. D., and Thomson, S. A. (2001) Preliminary studies in the formation of ethyl methylphosphonofluoridate from rat and human serum exposed to VX and treated with fluoride ion. *Anal. Lett. 34*, 727−737.

(34) Matsuda, Y., Nagao, M., Takatori, T., Niijima, H., Nakajima, M., Iwase, H., Kobayashi, M., and Iwadate, K. (1998) Detection of the

sarin hydrolysis product in formalin-fixed brain tissues of victims of the Tokyo subway terrorist attack. *Toxicol. Appl. Pharmacol. 150*, 310−320.

(35) Nagao, M., Takatori, T., Matsuda, Y., Nakajima, M., Iwase, H., and Iwadate, K. (1997) Definitive evidence for the acute sarin poisoning diagnosis in the Tokyo subway. *Toxicol. Appl. Pharmacol. 144*, 193−203.

(36) Polhuijs, M., Langenberg, J. P. and Benschop, H. P. (1997) New method for retrospective detection of exposure to organophosphorus anticholinesterases: application to alleged sarin victims of Japanese terrorists. *Toxicol. Appl. Pharmacol. 146*, 156−161.

(37) van der Schans, M. J., Polhuijs, M., van Dijk, C., Degenhardt, C. E., Pleijsier, K., Langenberg, J. P., and Benchop, H. P. (2004) Retrospective detection of exposure to nerve agents: analysis of phosphofluoridates originating from fluoride-induced reactivation of phosphylated BuChE. *Arch. Toxicol. 78*, 508−524.

(38) George, K. M., Schule, T., Sandoval, L. E., Jennings, L. L., Taylor, P., and Thompson, C. M. (2003) Differentiation between acetylcholinesterase and the organophosphate-inhibited form using antibodies and the correlation of antibody recognition with reactivation mechanism and rate. *J. Biol. Chem. 278*, 45512−45518.

(39) Tsuge, K., and Seto, Y. (2006) Detection of human butyrylcholinesterase-nerve gas adducts by liquid chromatography−mass spectrometric analysis after in gel chymotryptic digestion. *J. Chromatogr., B 838*, 21−30.

(40) Noort, D., Fidder, A., van der Schans, M. J., and Hulst, A. G. (2006) Verification of exposure to organophosphates: generic mass spectrometric method for detection of human butyrylcholinesterase adducts. *Anal. Chem. 78*, 6640−6644.

TX600310Y